EPJ Web of Conferences **303**, 01020 (2024) https://doi.org/10.1051/epjconf/202430301020
MENU 2023

The light baryon resonance spectrum in a coupled-channel approach – Recent results of the Jülich-Bonn model

Deborah Rönchen[1,*]

[1]Institute for Advanced Simulation Forschungszentrum Jülich, 52425 Jülich, Germany

Abstract. We present recent results from the Jülich-Bonn dynamical coupled-channel approach, where the spectrum of nucleon and Delta resonances is extracted based on a combined study of the pion- and photon-induced production of πN, ηN, $K\Lambda$ and $K\Sigma$ final states. The amplitudes of the Jülich-Bonn model also enter the study of electroproduction reactions as constraints at $Q^2 = 0$.

1 Introduction

The spectrum of baryon resonances encodes the key to understanding the strong force at medium energies and the determination of the excited states is a long-term experimental and theoretical challenge. It is complicated by the fact that light baryon resonances are often overlapping, sometimes very broad and do not appear as distinct peaks in cross section data. In order to connect predictions for the baryon spectrum in the non-perturbative energy regime from quark models or lattice calculations to experimental data, coupled-channel frameworks are especially suited. They take into account the opening of the various inelastic channels in the energy regime of interest. In those approaches a simultaneous partial-wave analysis of multiple reactions with different initial and final states is performed, followed by a pole search in the scattering amplitudes. Those poles represent the resonance states, the coupling strength to the different channels is characterized by the residues.

The Jülich-Bonn dynamical coupled-channel (JüBo DCC) model is a theoretically well-defined approach based on the meson exchange picture, which respects (2-body) unitarity and analyticity. The latter is an essential requirement for a reliable extraction of the resonance spectrum in terms of pole positions in the complex energy plane [1]. Originally formulated to describe elastic πN scattering [2], it has been extended to a number of different hadronic final states [3–5], to photon-induced reactions [6–9] and also to the hidden charm sector [10] in the last years. Moreover, the framework was recently adapted to electroproduction reactions in the Jülich-Bonn-Washington (JBW) parameterization [11–13]. In Ref. [14] the nature of N^* and Δ resonances was studied within the JüBo model with regard to whether they are compact states formed by quarks and gluons, or hadronic molecules generated from the meson-baryon interaction.

*e-mail: d.roenchen@fz-juelich.de

2 Theoretical formalism

In the JüBo model the hadronic meson-baryon interaction is described by a scattering matrix T which obeys the following scattering equation, formulated in time-ordered perturbation theory and partial-wave basis:

$$T_{\mu\nu}(q, p', W) = V_{\mu\nu}(q, p', W) + \sum_{\kappa} \int_0^\infty dp\, p^2\, V_{\mu\kappa}(q, p, W) G_\kappa(p, W)\, T_{\kappa\nu}(p, p', W)\,. \quad (1)$$

Here, W is the scattering energy in the center-off-mass system and q (p, p') is the modulus of the outgoing (intermediate, incoming) momentum. Off-shell momenta are included in the integral. $V_{\mu\nu}$ stands for the driving transition amplitude from the initial meson-baryon channel ν to the final meson-baryon channel μ and contains unknown parameters. It is build of t- and u-channel exchanges of known mesons and baryons, s-channel pole terms to account for genuine resonances and phenomenological contact terms, see Refs. [3, 4, 7] for a complete list of exchange diagrams and the corresponding formulas. The dynamical generation of resonances without an explicit s-channel diagram is possible in the JüBo model. The scattering matrix T enters the calculation of observables that are fitted to experimental data, which determines the unknown parameters in $V_{\mu\nu}$. The model features the channels $\kappa = \pi N$, ηN, $K\Lambda$, $K\Sigma$, σN, ρN and $\pi\Delta$. The latter three channels account effectively for the three-body $\pi\pi N$ channel. They are included in the model by matching the corresponding $\pi\pi$ and πN phase shifts [2].

Photoproduction reactions are described in a semi-phenomenological approach with the photoproduction mutilpole amplitude given by

$$\mathcal{M}_{\mu\gamma}(q, W) = V_{\mu\gamma}(q, W) + \sum_{\kappa} \int_0^\infty dp\, p^2\, T_{\mu\kappa}(q, p, W) G_\kappa(p, W) V_{\kappa\gamma}(p, W)\,, \quad (2)$$

where $\mathcal{M}$ stands for an electric or magnetic multipole. The index γ stands for the initial γN channel with a real ($Q^2 = 0$) photon, and μ (κ) denotes the final (intermediate) meson-baryon pair. $T_{\mu\kappa}$ is the hadronic half-off-shell matrix of Eq. (1) with the off-shell momentum p and the on-shell momentum q, and $V_{\mu\gamma}$ stands for the driving photoproduction amplitude. In Eqs. (1) and (2), G_κ denotes the meson-baryon two-body propagator. As $V_{\mu\nu}$ of Eq. (1), $V_{\mu\gamma}$ contains unknown parameters that can only be determined in fits to experimental data. In contrast to the purely hadronic potential, the photo potential $V_{\mu\gamma}$ is not formulated in a field-theoretical description but approximated by energy-dependent polynomials:

$$V_{\mu\gamma}(p, W) = \alpha^{NP}_{\mu\gamma}(p, W) + \sum_i \frac{\gamma^a_{\mu;i}(p)\gamma_{\gamma;i}(W)}{W - m^b_i}\,, \quad (3)$$

where the quantities $\gamma_{\gamma;i}$ and $\alpha^{NP}_{\mu\gamma}$, which denote the photon resonance vertex and the photon coupling to the non-pole part, respectively, are parameterized phenomenologically as a polynomial function in energy W. The hadronic vertex function $\gamma^a_{\mu;i}$ is precisely the same as in the field-theoretical description of the hadronic reactions [4] and also enters Eq. (1). This parameterization of the photproduction process is of numerical advantage since the evaluation time is a critical point for a model with a large number of fit parameters.

3 Recent results from an analysis of photoproduction reactions

In the most recent version "JüBo2022" [9], the JüBo model was extended to $K\Sigma$ photoproduction off the proton. A simultaneous analysis of the reactions $\pi N, \gamma p \to \pi N$, ηN, $K\Lambda$, $K\Sigma$

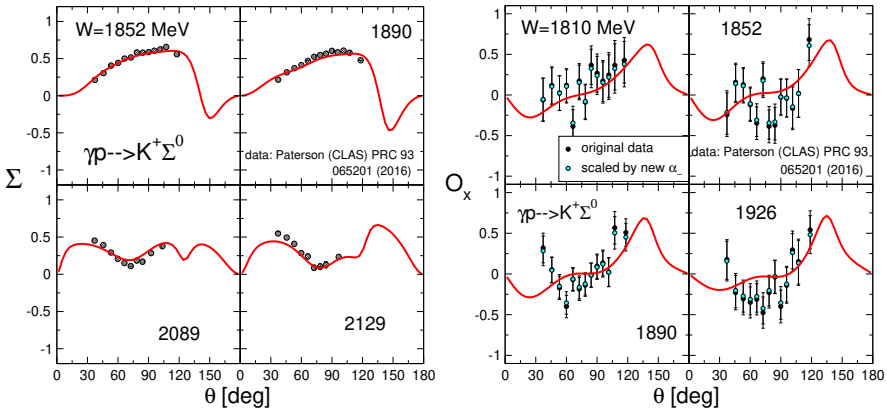

Figure 1. Selected fit results (red solid lines) for the reaction $\gamma p \to K^+\Sigma^0$: Beam asymmetry Σ (left) and beam-recoil polarization O_x (right). Data: CLAS Collaboration [17]. In case of O_x the data are scaled by the new value of the Λ decay parameter α_- [18].

was performed. About 900 free parameters were adjusted to almost 72,000 data points using the supercomputer JURECA at the Jülich Supercomputing Centre [15]. Selected fit results are shown in Fig. 1. A complete list of all included experimental data and the corresponding fit results can be found online [16].

Pole positions of all N^* and Δ resonances rated with four stars by the Particle Data Group up to a total spin of $J = 9/2$ could be determined. One exception is the $N(1895)1/2^-$ which is not included in the approach. In addition we find states rated with less than four stars, see Ref. [9] for a complete list. Compared to our previous analysis [8] which included $K\Lambda$ but not $K\Sigma$ photoproduction, no new genuine s-channel resonances had to be incorporated, but we see indications for new dynamically generated states in the D_{13}, D_{33} and G_{39} partial waves. However, further evidence for the existence of those states is needed.

The analysis of the partial-wave content shows that the reaction $\gamma p \to K^+\Sigma^0$ is dominated by isospin $I = 3/2$ partial waves, with the exception of the P_{13} wave, c.f. Fig. 2. This partial wave features two resonance states, the $N(1720)3/2^+$ and the $N(1900)3/2^+$. New data from the BGOOD experiment [19] show a drop in the cross section at forward angles around $W \sim 1900$ MeV. In our analysis this behavior is closely related to the $N(1900)3/2^+$. Although the cusp-like structure in the left-hand plot of Fig. 2 can only be qualitatively described, we achieve a good description of the data from the same measurement [19] with a higher angular resolution (right-hand plot of Fig. 2). Note that only the latter data set is included in the fit. Accordingly, we observe significant changes in the resonance parameters of the two states in the P_{13} wave compared to our previous analysis [8] where the recent BGOOD data were not included, see Tab. 1.

Recent data for other channels as, e.g., new measurements in eta photoproduction off the proton by the CBELSA/TAPS collaboration [21, 22] were also newly included in the JüBo2022 analysis. Among those, the inclusion of the new data on the polarization observables T, E, P, H, and G [22] resulted in a much larger ηN residue of the $N(1650)1/2^-$ compared to previous studies, c.f. Tab. 2. This reduces the striking difference in the ηN residues of the two S_{11} states $N(1535)1/2^-$ and $N(1650)1/2^-$. A similar observation was also made in an analysis of the same data by the Bonn-Gatchina group [22].

The impact of this recent measurement on the resonance parameters reinforces the need for polarization observables to reliably determine the spectrum. This applies especially to the

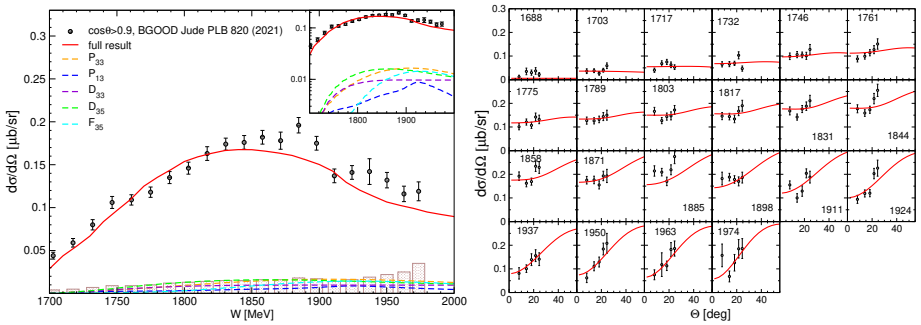

Figure 2. Differential cross section in forward direction for the reaction $\gamma p \to K^+\Sigma^0$. Data: T. Jude *et al.* (BGOOD) [19]. Only the data in the right-hand plot with a higher angular resolution are included in the fit. (Figures originally published in Ref. [9].)

Table 1. Resonance parameters of P_{13} states from the recent JüBo2022 analysis [9], compared to the previous JüBo2017 analysis [8] and the estimates of the Particle Data Group ("PDG") [20]: Pole positions W_0 ($\Gamma_{\rm tot}$ defined as -2ImW_0) and normalized residue ($\sqrt{\Gamma_{\pi N}\Gamma_{K\Sigma}}/\Gamma_{\rm tot}, \theta_{\pi N\to K\Sigma}$) of the $K\Sigma$ channel.

		Re W_0	-2Im W_0	$\frac{\Gamma_{\pi N}^{1/2}\Gamma_{K\Sigma}^{1/2}}{\Gamma_{\rm tot}}$	$\theta_{\pi N\to K\Sigma}$
		[MeV]	[MeV]	[%]	[deg]
$N(1720)\ 3/2^+$	2022	1726(8)	185(12)	5.9(1)	82(6)
	2017	1689(4)	191(3)	0.6(0.4)	26(58)
	PDG 2022	1675 ± 15	250^{+150}_{-100}	—	—
$N(1900)\ 3/2^+$	2022	1905(3)	93(4)	1.3(0.3)	$-40(18)$
	2017	1923(2)	217(23)	10(7)	$-34(74)$
	PDG 2022	1920±20	150±50	4±2	110±30

pion-induced channels like $\pi N \to KY$ where the data quality and quantity is in general only poor, but also to photoproduction channels like $K^0\Sigma^+$, where only very few polarization data are available so far. Accordingly, a recent update of the JüBo analysis with new double polarization observables by the CLAS Collaboration [23] for $\gamma p \to K^0\Sigma^+$ resulted in significant changes of the pole positions for some states.

4 Electroproduction reactions in the Jülich-Bonn-Washington parameterization

The amplitudes of the Jülich-Bonn model described in the previous sections also enter the study of electroproduction reactions as constraints at $Q^2 = 0$. In the so-called Jülich-Bonn-Washington (JBW) parameterization [11] the photoproduction multipole amplitude of Eq. (2) is extended to virtual photons. To this end, the electroproduction potential $V_{\mu\gamma^*}(p, W, Q^2)$ is parameterized as

$$V_{\mu\gamma^*}(p, W, Q^2) = \alpha^{NP}_{\mu\gamma^*}(p, W, Q^2) + \sum_i \frac{\gamma^a_{\mu;i}(p)\gamma_{\gamma^*;i}(W, Q^2)}{W - m^b_i} \,. \tag{4}$$

Table 2. Resonance parameters of the S_{11} states from the recent JüBo2022 analysis [9], compared to the previous JüBo2017 analysis [8] and the estimates of the Particle Data Group ("PDG") [20]: Pole positions W_0 ($\Gamma_{\rm tot}$ defined as -2ImW_0) and normalized residue ($\sqrt{\Gamma_{\pi N}\Gamma_{\eta N}}/\Gamma_{\rm tot}, \theta_{\pi N\to\eta N}$) of the ηN channel.

		Re W_0	-2Im W_0	$\frac{\Gamma_{\pi N}^{1/2}\Gamma_{\eta N}^{1/2}}{\Gamma_{\rm tot}}$	$\theta_{\pi N\to\eta N}$
		[MeV]	[MeV]	[%]	[deg]
$N(1535)\ 1/2^-$	2022	1504(0)	74 (1)	50(3)	118(3)
	2017	1495(2)	112(1)	51(1)	105(3)
	PDG 2022	1510 ± 10	130 ± 20	43 ± 3	−76 ± 5
$N(1650)\ 1/2^-$	2022	1678(3)	127(3)	34(12)	71(45)
	2017	1674(3)	130(9)	18(3)	28(5)
	PDG 2022	1655 ± 15	135 ± 35	29 ± 3	134 ± 10

The Q^2 dependence is introduced in a separable form:

$$\alpha^{NP}_{\mu\gamma^*}(p,W,Q^2) = \tilde{F}^{\mu}(Q^2)\alpha^{NP}_{\mu\gamma}(p,W) \quad \text{and} \quad \gamma_{\gamma^*;i}(W,Q^2) = \tilde{F}_i(Q^2)\gamma_{\gamma;i}(W)\,, \tag{5}$$

with one channel-dependent form-factor $\tilde{F}^{\mu}(Q^2)$ and another channel-independent form-factor $\tilde{F}_i(Q^2)$ that depends on the resonance number i. The quantities $\alpha^{NP}_{\mu\gamma}$ and $\gamma_{\gamma;i}$ are the same as in Eq. (3), i.e. parameterized as polynomials. Constraints from gauge invariance are included by explicitly implementing Siegert's theorem [24].

A detailed description of the JBW approach is given in Ref. [11] where pion electroproduction was analyzed. The framework was extended to eta electroproduction in Ref. [12]. In Ref. [13] the first ever coupled-channel study of pion, eta and $K\Lambda$ electroproduction off the proton was achieved. Here, 533 fit parameters were adjusted to more than 110.000 data points in a kinematic range of $W < 1.8$ GeV and $Q^2 < 8$ GeV^2. The input at the photon point $Q^2 = 0$ was taken from the JüBo2017 solution.

The JBW formulation ensures universal pole positions and residues in the electro-, photo- and purely hadronic amplitudes and is designed for the long-term goal to extract resonance parameters in a simultaneous analysis of all three production mechanisms.

Acknowledgments

This work has been carried out in collaboration with M. Döring, J. Hergenrather, M. Mai, T. Mart, Ulf-G. Meißner, C.-W. Shen, Y.-F. Wang, and R. Workman. This work is supported by DFG and NSFC through funds provided to the Sino-German CRC 110 "Symmetry and the Emergence of Structure in QCD" (NSFC Grant No. 11621131001, DFG Grant No. TRR110) and by the MKW NRW under the funding code NW21-024-A. The authors gratefully acknowledge computing time on the supercomputer JURECA [15] at Forschungszentrum Jülich under grant no. "baryonspectro".

References

[1] M. Döring *et al.*, Nucl. Phys. A **829**, 170 (2009).
[2] C. Schütz, J. W. Durso, K. Holinde and J. Speth, Phys. Rev. C **49**, 2671-2687 (1994).
[3] M. Döring *et al.*, Nucl. Phys. A **851**, 58 (2011).

[4] D. Rönchen, M. Döring, F. Huang, H. Haberzettl, J. Haidenbauer, C. Hanhart, S. Krewald, U.-G. Meißner, K. Nakayama, Eur. Phys. J. A **49**, 44 (2013).
[5] Y.-F. Wang, D. Rönchen, U.-G. Meißner, Y.-Lu, C.-W. Shen and J.-J. Wu, Phys. Rev. D **106**, no.9, 094031 (2022).
[6] D. Rönchen, M. Döring, F. Huang, H. Haberzettl, J. Haidenbauer, C. Hanhart, S. Krewald, U.-G. Meißner and K. Nakayama, Eur. Phys. J. A **50**, 101 (2014).
[7] D. Rönchen, M. Döring, H. Haberzettl, J. Haidenbauer, U.-G. Meißner and K. Nakayama, Eur. Phys. J. A **51**, 70 (2015).
[8] D. Rönchen, M. Döring, U.-G. Meißner, Eur. Phys. J. A **54**, 110 (2018).
[9] D. Rönchen, M. Döring, U.-G. Meißner and C.-W. Shen, Eur. Phys. J. A **58**, 229 (2022).
[10] Z.-L. Wang, C.-W. Shen, D. Rönchen, U.-G. Meißner and B.-S. Zou, Eur. Phys. J. C **82**, no.5, 497 (2022).
[11] M. Mai *et al.* [Jülich-Bonn-Washington], Phys. Rev. C **103**, 65204 (2021).
[12] M. Mai *et al.* [Jülich-Bonn-Washington], Phys. Rev. C **106**, 015201 (2021).
[13] M. Mai *et al.* [Jülich-Bonn-Washington], Eur. Phys. J. A **59**, no.12, 286 (2023).
[14] Y.-F. Wang, U.-G. Meißner, D. Rönchen and C.-W. Shen, Phys. Rev. C **109**, no.1, 015202 (2024).
[15] Jülich Supercomputing Centre, Journal of large-scale research facilities, 7, A182 (2021).
[16] Figures representing the full fit result of this study, including a display of all data, can be downloaded at http://collaborations.fz-juelich.de/ikp/meson-baryon/main.
[17] C. A. Paterson *et al.* [CLAS], Phys. Rev. C **93**, no.6, 065201 (2016).
[18] D. G. Ireland, M. Döring, D. I. Glazier, J. Haidenbauer, M. Mai, R. Murray-Smith and D. Rönchen, Phys. Rev. Lett. **123**, no.18, 182301 (2019).
[19] T. C. Jude, S. Alef, P. Bauer, D. Bayadilov, R. Beck, A. Bella, J. Bieling, A. Braghieri, P. L. Cole and D. Elsner, *et al.* Phys. Lett. B **820**, 136559 (2021).
[20] R. L. Workman *et al.* [Particle Data Group], PTEP **2022**, 083C01 (2022).
[21] F. Afzal *et al.* [CBELSA/TAPS], Phys. Rev. Lett. **125**, no.15, 152002 (2020).
[22] J. Müller *et al.* [CBELSA/TAPS], Phys. Lett. B **803**, 135323 (2020).
[23] L. Clark *et al.* [CLAS], [arXiv:2404.19404 [nucl-ex]].
[24] A. J. F. Siegert, Phys. Rev. **52**, 787 (1937).